Estuaries and Coasts
https://doi.org/10.1007/s12237-020-00785-2

Nitrogen and Phosphorus Export After Flooding of Agricultural Land by Coastal Managed Realignment

Erik Kristensen[1] · Cintia O. Quintana[1] · Thomas Valdemarsen[1] · Mogens R. Flindt[1]

Received: 15 December 2019 / Revised: 18 May 2020 / Accepted: 16 June 2020

Abstract

Climate-driven sea level rise has severe consequences for drained agricultural areas near coasts. The least productive of these can be restored into marine wetlands of high ecological quality by managed realignment. This study assessed the nitrogen (N) and phosphorus (P) balance in a 214 ha coastal lagoon formed after flooding of agricultural land by managed realignment. N and P loss from the soils was monitored over a 5-year period after flooding using three independent approaches: (1) temporal changes in N and P inventories of the soil; (2) flux of dissolved inorganic N and P from the flooded soil; and (3) tidal N and P exchange across the outer boundary in the form of particulate and dissolved nutrients. All three approaches showed similar initial release and tidal export of N and P the first year(s) after flooding followed by decreasing rates. The annual loss ranged from 157 to 299 kg N ha^{-1} yr^{-1} and 29 to 63 kg P ha^{-1} yr^{-1} during the first year. N loss decreased rapidly after the first 2 years and reached a level of 28–65 kg N ha^{-1} yr^{-1}, while P loss declined after the first year and remained stable and relatively high at 18–32 kg P ha^{-1} yr^{-1} thereafter. High N and P export after implementing managed realignment of agricultural land may deteriorate environmental conditions in the adjacent marine recipients for at least 5 years. Particularly small and stagnant water bodies vulnerable to eutrophication should be avoided as recipients.

Keywords Gyldensteen Coastal Lagoon · N and P · Soil inventories · Soil-water flux · Tidal export

Introduction

Marine and terrestrial ecosystems along coastlines are increasingly impacted by anthropogenic activities. Eutrophication and climate change are currently among the most critical human stressors (Chapman 2017; Meier et al. 2017; Smith et al. 2017). Deleterious effects of coastal eutrophication are well-documented and have been subject to considerable research and mitigation efforts for the last few decades (Paerl et al. 2014; Hale et al. 2016; Lefcheck et al. 2017). Conversely, climate change impacts on ecosystems at the sea-land interface by sea level rise and increasing storm intensity are relatively recent and less well-studied (IPCC 2014; Smith et al. 2017; Schuerch et al. 2018).

Climate change has large ecological and economic consequences when coastal defenses (e.g., dikes) are weakened by sea level rise and disastrously breached by intensifying storms causing severe flooding of the low-lying hinterland (Hall et al. 2006; Woodruff et al. 2013). Areas threatened by flooding should be protected by reinforcement of coastal defenses when they accommodate businesses and infrastructure of economic importance for human populations or terrestrial ecosystems of high ecological value (Arnbjerg-Nielsen et al. 2015; Vousdoukas et al. 2018). However, not all low-lying inland areas prone to flooding have sufficient economic and ecological value to warrant investments in costly coastal defenses. In fact, many economically inferior agricultural areas near coasts are hard to cultivate and not worth protecting, particularly reclaimed seabeds that were drained and diked more than a century ago (Esteves 2014). For example, land reclamations drained 450 km^2 of seabed in the shallow inner waters and fjords around Denmark for agricultural purposes during the nineteenth century (Stenak 2005; Fenger et al. 2008; Hansen 2008). Many of these drained soils have through time subsided into moist meadows and are protected by vulnerable dikes that must be reinforced considerably to withstand the projected sea level rise of about 1 m by year 2100 (Hansen

Communicated by Hans W. Paerl

✉ Erik Kristensen
ebk@biology.sdu.dk

[1] Department of Biology, University of Southern Denmark, Odense, Denmark

Published online: 22 June 2020

2008; IPCC 2019). Cost-benefit analyses reveal that the least productive of these agricultural areas easily can be restored into shallow marine wetlands of high ecological and recreational quality by managed realignment (French 2006; Esteves 2014).

Managed realignment involves deliberate breaching of older engineered defenses to allow the coastline to migrate landward (French 2006; Rupp-Armstrong and Nicholls 2007). The benefits include increased wave attenuation and reduction of storm impacts due to the increased tidal volume of the new flooded area (Esteves 2014). Managed realignment not only provides a sustainable new line of coastal defense but also creates new coastal ecosystems with a potential high value for marine biodiversity and bird wildlife (Mander et al. 2013; Brady and Boda 2017). The approach has over the past couple of decades become more common, but the knowledge of its physicochemical, biogeochemical, and ecological implications is still limited (Pétillon et al. 2014; Spencer et al. 2017; Dale et al. 2019).

While some studies have examined how managed realignment affects hydrodynamics, erosion, particle transport, and sediment geochemistry as well as flora and fauna succession (Burton et al. 2011; Dale et al. 2017), less is known about the release and tidal exchange of nutrients from agricultural land newly flooded by seawater (Ardón et al. 2017). Only a few studies have examined the nitrogen (N) and phosphorus (P) export at managed realignment sites, and they are mostly focused on sequestering based on sedimentation and accretion in restored saltmarshes (Andrews et al. 2008; Burden et al. 2013). Agricultural soils accumulate labile and exchangeable N and P compounds during cultivation (Heyburn et al. 2017; Wironen et al. 2018), which may be rapidly released by chemical and biogeochemical processes after flooding with seawater (Portnoy and Giblin 1997; Ardón et al. 2013). Two obvious questions arise in this respect—How easily exchangeable are the inventories of N and P in anoxic soil after flooding with seawater? And how fast will they be exhausted by soil processes and tidal exchange? Answers to these questions are important for understanding of the wider ecological implications of managed realignment. If flooded agricultural soil is a significant source of N and P nutrients to coastal areas vulnerable to eutrophication, it can have detrimental impacts on the recipient marine ecosystems.

The purpose of this study was to determine the N and P export from a new coastal lagoon formed after flooding of agricultural land by managed realignment. Focus was on N and P release from the soil and the associated ecological effects within the lagoon and in the adjacent water body. The temporal pattern of nutrient export from Gyldensteen Coastal Lagoon, Denmark, was followed the first 5 years after deliberate flooding of 214 ha farmland with seawater. The fate of exchangeable N and P in the flooded soil was determined using three independent approaches: 1) Temporal changes in the N and P inventory of the soil; 2) Diffusive release of dissolved inorganic N and P from the flooded soil; and 3) Tidal N and P exchange across the outer boundary of the lagoon in the form of plant detritus, fine particles and dissolved nutrients. The hypotheses were that 1) Excess nutrients stored in the soil from past fertilization is rapidly lost under anoxic and saline conditions induced by flooding; and 2) N and P loss to the adjacent ocean attenuates similarly within the first few years after flooding.

Materials and Methods

Study Site

Samplings for determination of soil/water nutrient dynamics were conducted from 2014 to 2019 in the newly flooded Gyldensteen Coastal Lagoon located along the northern coast of Fyn island, Denmark (Fig. 1). The lagoon was established (or restored) by managed coastal realignment of 214 ha agricultural land on 29 March 2014. The area is originally an old marine lagoon that was diked and drained around 1870 and since then used for agricultural purposes (Stenak 2005). The cultivated soil was used for cattle grazing until ~1960 when more efficient draining allowed intensive cultivation of particularly barley, onion and leaks (Hansen 2014). The soil therefore received considerable amounts of nitrogen (N) and phosphorus (P) in the form of inorganic (chemical) and organic (manure) fertilizers from 1960 until 2013, although with lower intensity during the last few years before flooding in 2014 (Table 1). Analysis of the cultivated area has disclosed that many years of agricultural plowing has homogenized the soil texture to 0.2–0.3 m depth on top of the impermeable and clay-rich moraine subsoil typically found in the eastern part of Denmark (Wessel et al. 2019).

The new coastal lagoon is shallow (mean depth about 1 m) and microtidal (about ±20 cm), but occasionally with larger water level fluctuations (up to ±100 cm) during exceptional wind events. The tidal water enters and exits the lagoon through three openings (Fig. 1), with most water exchange in the deep western opening. Water salinity and temperature in the lagoon follows that in the ambient Kattegat marine environment, with salinity ranging from 20 to 30 and temperature from a winter low of ~0 °C to a summer high of 20–25 °C. There are no freshwater inputs to the system, except for a few minor agricultural drainage channels in the southern part. The marine area just outside the lagoon is shallow with water depths of 0.5–1 m several hundred meters offshore.

Algal development in the lagoon was monitored from 2014 to 2018 (Sandra W. Thorsen, unpublished). Briefly, after an initial short coverage of cyanobacteria in spring and early summer of 2014, a massive bloom of opportunistic green macroalgae (*Enteromorpha* spp., *Ulva* spp. and *Cladophora*

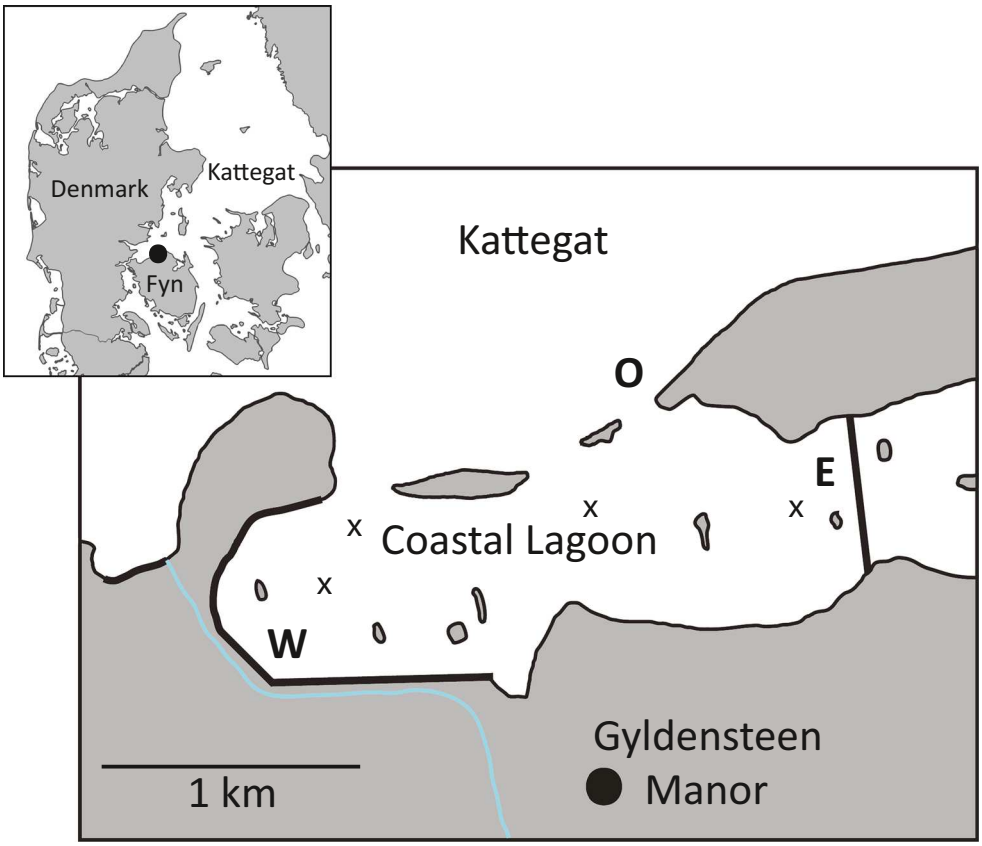

Fig. 1 Map of Gyldensteen Coastal Lagoon (571800 E, 6159300 N) with the major sampling stations West (W), East (E), and Outer (O) indicated. Crosses show the position of supplementary stations (from left to right: GI05, GI08, GI21, and GI28) for soil sampling

spp.) developed in the eastern part during late summer that year – a few months after flooding (Fig. 2). Surprisingly, no such blooms were evident in 2015 and most of 2016, where there was a low and even coverage of up to 11 species of green, red and brown macroalgae. In late summer of 2016 and during the entire year of 2017, a massive bloom of cyanobacteria covered all surfaces in the entire lagoon with a layer of up 1 cm in thickness. The cyanobacteria almost disappeared in winter 2017–18 and later in 2018 and 2019 the system had low coverage of cyanobacteria and similar high species diversity of macroalgae as experienced in 2015.

Table 1 Annual N and P fertilizer application to the 214 ha farmland that was flooded with seawater in 2014. The fertilizers used were of both manure and synthetic origin. The 2011 values represent the typical amounts applied every year in the preceding decades, while the 2012 and 2013 values show the lowered application intensity in order to prepare for the flooding. Data are from the fertilization log that was kindly provided by Gyldensteen Manor

Year	Ton N	Ton P
2011	34.4	4.3
2012	30.1	0.5
2013	11.7	0

Temporal Changes in Soil N and P Pools

The temporal development of soil characteristics in Gyldensteen Coastal Lagoon was determined from 20-cm deep soil cores sampled after flooding in May 2014, 2015, 2016, and 2018 (no sampling in 2017 and 2019). Triplicate soil cores were taken with 5 cm i.d. core tubes at each of 4–6 stations scattered across the lagoon; representing the major soil types. The 4 stations (GI05, GI08, GI21, and GI28) sampled in excess of the two main stations W and E are indicated from left to right by unlabeled crosses in Fig. 1. Unfortunately, no cores were sampled at GI05 and GI21 in 2014 and 2015. All cores were extruded in the laboratory and homogenized before subsamples were analyzed for grain size using a Malvern Mastersizer 3000 Particle Size Analyzer. Other subsamples were dried at 105 °C for 24 h and ground into powder before the total nitrogen (TN) content was determined with a Thermo Analytical elemental analyzer, Flash EA 2000. Subsamples of the dried soil were combusted at 520 °C for 6 h, and total phosphorus (TP) and iron (TFe) were extracted by boiling the ash at 120 °C in 1 M HCl for 1 h. The extract was analyzed for dissolved inorganic phosphorus (DIP) and Fe^{2+} (after reduction with hydroxylamine) by colorimetric analysis (Stookey 1970; Koroleff, 1983).

Fig. 2 Photos showing the flora development at station E: 2014—green algal bloom; 2015—no algae (stubs of crops from 2013 visible); and 2017—cyanobacterial cover

Soil-Water Nutrient Fluxes

The release of dissolved inorganic nitrogen (DIN) and phosphorus (DIP) from soil to water at stations W and E was determined on a seasonal basis by in situ sealed benthic chamber incubations in January–February (winter), May (spring), July–August (summer), and October (fall) from summer 2014 to spring 2019. Three cylindrical flux chambers (40 cm i.d. and 20 cm deep) were deployed at each station one day before initiating the measurements. The chambers were pushed about 5 cm into the soil and left with open tops overnight. The next morning, all chambers were sealed and equipped individually with a stirrer motor driving a 5-cm long stirrer bar at about 120 rpm and covered by black plastic to prevent light intrusion. Water samples for DIN and DIP analyses were taken through an otherwise sealed sampling port in the lid at the start and end of incubation. The incubation time was 3 to 5 h depending on season and water temperature. Water samples were GF/C-filtered and frozen at −20 °C until DIN (= $NH_4^+ + NO_2^- + NO_3^-$) and DIP (= PO_4^{3-}) were analyzed on a Skalar SAN^{++} Analyzer System according to the manufacturer's guidelines. Fluxes were calculated as mmol m^{-2} day^{-1} by relating the change in concentration over time to the volume and area of flux chambers.

Surface Water Sampling and Analysis

Surface water samples for dissolved and fine-particulate nutrients were taken at three evenly distributed dates during each sampling month and reported as monthly averages. The frequency of these monthly samplings was selected once during summer and fall in 2014; all seasons in 2015; and winter and spring in 2016. Sampling frequency was from summer in 2016 increased to every month. Water samples of 10 l were taken at stations W and E inside the coastal lagoon and station O outside the lagoon during each sampling date (Fig. 1). After return to the laboratory, half of each water sample was GF/C-filtered and both filtered and unfiltered water was frozen at −20 °C until analysis for dissolved and particulate nutrients. Filtered water samples were analyzed for DIN and DIP as described above. Total nitrogen (TN) in unfiltered water samples was analyzed on a Shimadzu TOC-L equipped with a TNM-L Module. Total phosphorus (TP) in unfiltered water samples was determined as DIP by colorimetric analysis as described above after wet oxidation of samples in a 5% $K_2O_8S_2$ solution at 120 °C for 1 h. TN and TP in the water samples included both fine-particulate and dissolved organic (FPDN and FPDP), as well as dissolved inorganic (DIN and DIP) N and P pools.

Tidal Transport of Macro Detritus

The import and export of drifting macrophytes and other macro detritus driven by tidal- and wind-generated currents were quantified at the outer boundary of the lagoon. The measurements were performed once every season from early 2014 to early 2018. Three nets with a mesh size of 9 mm and a hydraulic area of 1.0 m^2 were at each sampling occasion placed across the major channel in the west during one full tidal cycle. All materials trapped by the nets were cleared off on an hourly basis and stored for identification and quantification

(Flindt et al. 1997, 2004). The nets were emptied more frequently (15 or 30 min) when and if accumulated macro detritus restricted water passage through the nets. The trapped materials were weighed on site, and subsamples were subsequently dried in the laboratory for determination of wet weight/dry weight conversions and analyzed for N and P content as described above.

Modeling of Nutrient Export and Import

A 2-D coupled hydrodynamic and transport/dispersion model was used for mass balance calculations. The hydrodynamic model, including a bathymetric description, was developed for determining the tidal exchange of particulate and dissolved N and P between Gyldensteen Coastal Lagoon and the adjacent marine environment. Bathymetric data was obtained from the Danish Elevation Model (DK-DEM) and corrected for construction of new dikes and other recent structures using local drone monitoring (COWI A/S). High precision of x, y, and z coordinates (extracted with a resolution of 10 cm) was used to define the exact bathymetry in the final digital elevation model (DEM-model). The diked landward boundary defined the circumference of the lagoon, while tidal connection through the three openings to the open Kattegat defined the outer boundary. The model area was expressed by a series of mass conservation and momentum calculations (Flindt and Kamp-Nielsen 1997).

The forcing function for the hydrodynamic model was based on water level measurements at the nearby meteorological monitoring station in Bogense Harbor (DMI, Station 28,003/4: 567878 E, 6158502 N). Temporal resolution of the water level measurements was 15 min. The hydrodynamic model was calibrated against two pressure transducers deployed inside the lagoon at stations W and E over shorter periods during the growth season (8 May to 17 September 2014). The near-bed roughness parameter (reciprocal Manning number) was calibrated to correct for remnant shrubs from past agriculture activities. The best calibration (Nash-Sutcliffe model efficiency coefficient, 0.63; correlation statistics, $r^2 = 0.98$, $P < 0.001$) appeared with a reciprocal Manning number of 12, indicating high sediment roughness. Validation was performed on a different time series (4 May to 27 September 2015) of forcing data, and the statistics was acceptable (Nash-Sutcliffe model efficiency coefficient, 0.63; correlation statistics, $r^2 = 0.96$, $P < 0.001$) (Nash and Sutcliffe 1970).

The outer boundary forcing functions for the transport/dispersion module were set according to N and P concentrations from the nearest national water quality monitoring station (Vej0006870; 568568 E, 6170355 N), where data was obtained every second week. The transport dispersion module was calibrated by stepwise changing the dispersion coefficient (Flindt and Kamp-Nielsen 1997) until the best fit between measured and simulated DIN concentrations ($r^2 = 0.94$; $P < 0.005$). The validation was also here performed using the alternative time series ($r^2 = 0.91$; $P < 0.005$). It would have been more optimal to calibrate against salinity (Flindt and Kamp-Nielsen 1997), but this was not possible because Gyldensteen Coastal Lagoon receives no freshwater runoff and therefore has no salinity gradient. From the outside national monitoring data and those measured inside the lagoon in this study, appropriate time series of DIN, DIP, FPDN, and FPDP concentrations was obtained, while the transported macrophytes and other macro detritus were captured directly at the boundary.

N and P mass balance at the outer boundary was calculated during each tidal cycle using the simulated water flow ($m^3\ s^{-1}$), current velocity ($m\ s^{-1}$), and the time series concentration of dissolved (DIN, DIP), fine particulate and dissolved organic (FPDN and FPDP), and captured macro detritus (Flindt et al. 2004). The cut-off between macro detritus and fine particles was here set to 9 mm as defined by the mesh used for capturing macro detritus. The obtained net transport of N and P was reported separately for the growth season (April to October) and the winter season (November to March).

Annual N and P Export

Annual nutrient release and export from Gyldensteen Coastal Lagoon to the surrounding marine environment was assessed from the data obtained above using three independent approaches: (1) area-integrated annual changes in 0–20 cm soil N and P inventories; (2) time- and area-integrated soil-water diffusive flux of DIN and DIP; and (3) time-integrated modeling of tidal N and P exchange across the outer boundary.

The annual loss in N and P inventories was estimated as the difference in the average 20-cm depth-integrated pools for the 4–6 sampling stations and extrapolated to the entire 214-ha area. Temporal changes in annual N and P loss were determined from May one year to May the next year for the period 2014 to 2018. Validity of the estimates relies on the assumptions that the selected sampling sites are representative for the entire lagoon and that the inventory changes occurring in the upper 20 cm account for most of the total soil loss of N and P. The uniform agricultural history of the flooded Gyldensteen Coastal Lagoon soils renders the chosen stations representative, and that the homogeneity of the plowing layer assures that the upper 20 cm is a reliable depth interval for N and P loss estimates (Wessel et al. 2019).

Seasonal DIN and DIP release from the flooded soil at station W and E was calculated as 3-month extrapolation of a single flux measurement about midway in each season. Annual export for the entire coastal lagoon from summer 2014 to spring 2019 was then estimated as the average sum of summer, fall, winter, and spring for the two measuring stations and extrapolated to the 214-ha area. The basic

assumptions are that a single mid-seasonal flux measurement is representative for the entire season and that the two measuring stations are representative for the entire lagoon. Since soil-water fluxes in each season are primarily controlled by temperature (Clavero et al. 2000; Serpetti et al. 2016), the former assumption is justified because the flux measurements were performed when the water was close to the seasonal median temperatures. The latter assumption is justified by the fact that most of the lagoon (> 90%) has similar agricultural history with respect to crops and fertilization.

The modeled tidal exchange of N and P on an annual basis from summer 2014 to spring 2018 was estimated as the sum of seasonal (summer, fall, winter, and spring) export by 3-month extrapolation of the mass balance obtained from one tidal cycle during each season. Such estimate is dependent on the assumption that the selected tidal cycle is representative for the entire season during which it was assessed (Etheridge et al. 2015). This is here justified by the selection of average tidal cycles midway between spring and neap tides during each season. Deviations from the typical tidal water level fluctuations by exceptional wind events were rare during the study period according to records from the Danish Meteorological Institute (Hansen 2018). Furthermore, the validity of extrapolating from three 1.0-m^2 nets in the western tidal channel to the entire outer boundary has been proved by Flindt et al. (1997, 2004).

Statistical Analysis

Two-way ANOVA was used to test for significant differences between time (2014 to 2019) and stations in soil TN and TP pools (W, E, GI08, and GI28) and soil-water nutrient fluxes (W and E). Stations GI05 and GI21 were not included in the statistical analysis of soil TN and TP pools since no data were available from 2014 and 2015. Normality and equality of variances were tested before the two-way ANOVA was performed. Tukey post hoc tests were applied to verify pairwise differences among factors. All statistical tests were performed with a significance level $\alpha = 0.05$ and using the software SigmaPlot 12.0.

Results

Soil TN and TP Inventories

The granulometry of the upper 20-cm soil at stations W and E changed from poorly sorted fine grained sand (median grain size of 0.07–0.1 mm) with high silt + clay content (35–50%) right after flooding in 2014 to medium sand with lower silt-clay content in 2018 (Table 2). The concentration of TN and TP in the soil varied among sampling stations and showed no significant change with depth in the upper 20 cm. The soil at stations W and E contained 37–60 and 55–66 μmol N $(g\ dw)^{-1}$, respectively, throughout the period from 2014 to 2018 (Table 2). The other sampled stations were near this range, except for a significantly higher level of 250–320 μmol N $(g\ dw)^{-1}$ at station GI08 that has never been cultivated. The soil TP was similar among all stations and ranged from 13 to 31 μmol P $(g\ dw)^{-1}$ with no consistent depth patterns. The N:P molar ratios of the total pools were below 5 and almost similar through time and location (Table 2), pointing toward excessive inventories of P in the soils. The TFe content was ~ 100 μmol $(g\ dw)^{-1}$ at both stations W and E with an increasing trend over time (Table 2).

The 0–20-cm depth-integrated inventories of TN and TP in the soil generally decreased over time at all stations (Table 3). The average annual decrease ranged from 1 to 7% of the standing inventory of TN and 1.5 to 4% of the TP inventory from 2014 to 2018. The decrease was significant at stations W, E, GI08, and GI28 for TN but not for TP. Despite the lack of statistical evidence for decreasing depth-integrated TP pools, there was a consistent trend at individual stations (e.g., station GI08 and E). The N:P ratio of the loss ranged from 5 to 24 and exceeded the bulk N:P ratios in the soil considerably. TN loss was most pronounced from May 2014 to May 2016, while TP loss was rapid only the first year (May 2014 to May 2015). Subsequently, annual loss was limited to 12–14% for TN (2017–18) and 33–39% for TP (2016–18) of the initial rapid rates.

Soil-Water Nutrient Fluxes

DIN and DIP were always released from soil to water at both station W and E. Both stations showed similar overall rates with the same significantly decreasing trend and variability of DIN release with time throughout the examined years (Fig. 3). DIN release varied seasonally with higher rates during summers (from 3 to 6 mmol $m^{-2}\ d^{-1}$ in 2014–15 to 1–2 mmol $m^{-2}\ d^{-1}$ in 2018–19) than the succeeding winters (from 1.5–3.4 mmol $m^{-2}\ d^{-1}$ in 2014–15 to 0.2–0.5 mmol $m^{-2}\ d^{-1}$ in 2018–19). DIN release was always dominated by NH_4^+ with a contribution of > 60% in spring and summer, while NO_3^- was consistently taken up at a low rate by the soil in fall and winter. DIP release varied in an unpredictable pattern with no significant trend among years and between stations W and E (Fig. 3). DIP varied seasonally at both stations with generally higher rates in summers (range from 0.1 to 1.0 mmol $m^{-2}\ d^{-1}$) than winters (range from 0 to 0.4 mmol $m^{-2}\ d^{-1}$).

Nutrients in the Water Column

The water column inside Gyldensteen Coastal Lagoon initially showed high DIN and DIP concentrations that gradually leveled off through time (Fig. 4). DIN always accumulated during the cold and dark winter season with highest

Table 2 Key solid phase parameters of the soils at stations W and E after the flooding in 2014 and 2018. The results are given as the average ± sd ($n = 3$) of pooled values in the upper 20 cm of the soil

		Station W				Station E			
		2014		2018		2014		2018	
		avg	sd	avg	sd	avg	sd	avg	sd
Median grain size	mm	0.118	0.007	0.147	0.016	0.067	0.010	0.137	0.011
Silt + clay	%	35.1	2.6	23.7	4.0	49.8	4.9	26.7	3.6
Total N	μmol g^{-1}	59.8	3.6	37.3	10.3	66.1	7.7	54.6	5.3
Total P	μmol g^{-1}	13.9	0.7	12.7	0.6	18.8	1.2	15.7	0.8
N:P		4.3:1		2.9:1		3.5:1		3.5:1	
Total Fe	μmol g^{-1}	69.1	3.3	134.4	0.7	101.5	0.2	104.8	6.2

concentrations at stations W and E in January 2015 reaching 52–55 μM. During the following years, the winter maximum gradually decreased to 27–36 μM in February 2016, ~ 21 μM in January 2017, and ~ 14 μM in January 2018. Although consumption by primary producers lowered DIN concentrations during summer inside the lagoon, the levels were still remarkably high during the first years with concentrations of 1–8 μM in summer 2014, 2–5 μM in summer 2015, and 1–7 μM in summer 2016. Later, in the summers of 2017 and 2018, the levels dropped to 0.5–1.5 μM. DIN levels at the outer boundary (station O) showed relatively stable fluctuations with winter maxima of 10–22 μM and summer minima of 2–4 μM in 2014–2016 and 0.2–0.4 μM in 2017–2018. Accordingly, the DIN concentrations at stations W and E were similar to those at Station O in winter of 2016–17 and even slightly lower in winter of 2017–18. DIN was mostly composed of NH_4^+ during the summer minima at all three sampled stations (Fig. 5), particularly in 2014 to 2016 where DIN almost exclusively consisted of NH_4^+. This summer trend gradually changed in 2017 and 2018 with much higher summer contribution of NO_3^- (> 40%). The winter DIN maxima were always dominated by NO_3^- (> 70%).

Table 3 Changes in inventories of total nitrogen (TN) and phosphorus (TP) in the upper 20 cm of soil sampled in May from 2013 to 2018 (except for 2017) at 4–6 stations in Gyldensteen Coastal Lagoon

	May 2014		May 2015		May 2016		May 2018	
	0–20 cm	sd	0–20 cm	sd	0–20 cm	sd	0–20 cm	sd
mol TN m^{-2}								
West	18.2	1.1	15.2	1.3	14.2	0.3	10.2	2.8
GI05	-		-		20.1	1.2	21.8	1.2
GI08	50.7	1.6	43.5	4.2	44.8	7.9	48.4	6.4
GI21	-		-		24.9	2.7	25.3	0.9
East	20.6	2.4	21.9	0.6	18.5	0.5	17.6	1.7
GI28	19.9	1.6	21.2	1.1	19.9	0.3	16.0	1.8
Average	27.4	15.6	25.4	12.4	23.7	10.9	23.2	13.4
Annual loss			2.0		1.7		0.25	
mol TP m^{-2}								
West	4.32	0.22	4.34	0.07	4.40	0.21	4.31	0.22
GI05	-		-		3.80	0.64	3.66	0.09
GI08	2.83	0.14	2.89	0.48	2.77	0.53	2.70	0.24
GI21	-		-		3.77	0.67	3.95	0.17
East	6.23	0.12	5.36	0.14	5.48	0.33	5.28	0.28
GI28	3.99	0.97	4.05	0.21	4.31	0.03	3.91	0.36
Average	4.34	1.41	4.16	1.02	4.09	0.90	3.97	0.84
Annual loss			0.18		0.07		0.06	

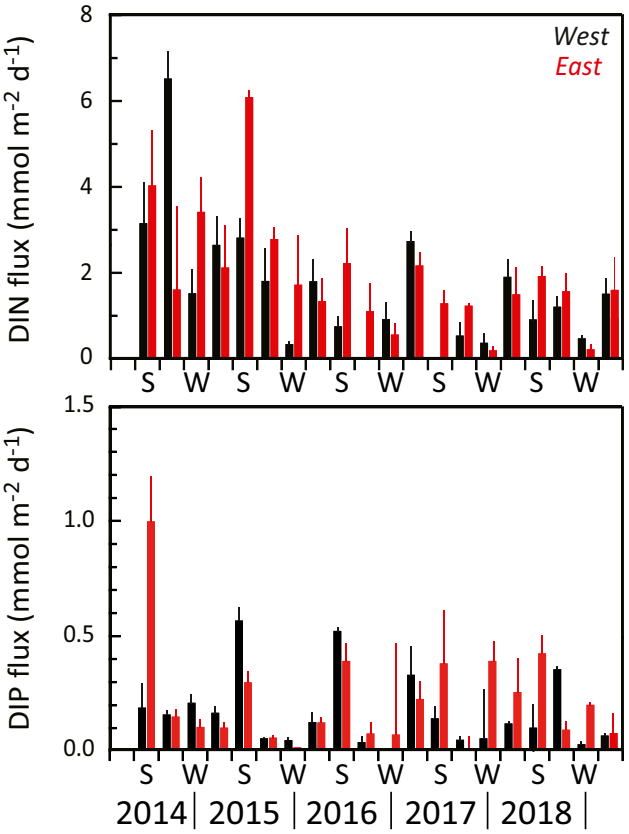

Fig. 3 DIN (upper) and DIP (lower) dark fluxes across the soil-water interface measured at 3–4-month intervals from summer 2014 to spring 2019. Black bars show results from station W and red bars from station E. Error bars indicate SE ($n = 3$)

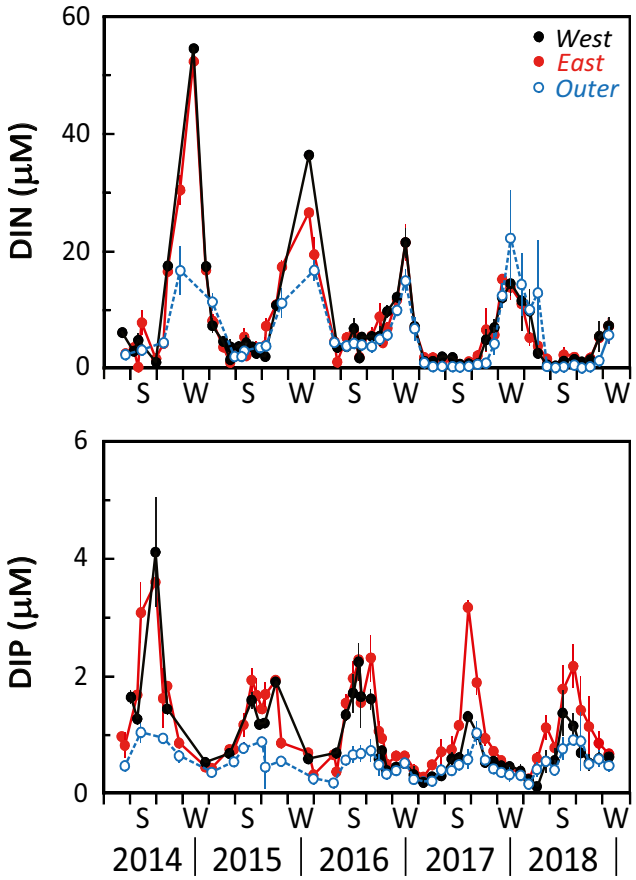

Fig. 4 DIN (upper) and DIP (lower) concentrations in lagoon water presented in 1–3-month intervals from May 2014 to June 2016 followed by monthly intervals until December 2018. Black symbols show results from station W; red symbols from station E; and blue symbols from station O. Error bars indicate SE ($n = 3$–5 until June 2016 and $n = 3$ until December 2018)

DIP always peaked during summer and early fall with highest concentrations of 3.6–4.1 µM at stations W and E in July 2014 (Fig. 4). Subsequently, the summer maxima decreased and remained roughly half of that level in 2015 (1.6–1.9 µM), 2016 (2.2–2.3 µM), 2017 (1.3–3.2 µM), and 2018 (1.4–2.2 µM). DIP minima occurred during early spring (March-April) in all years with concentrations around 0.2–0.4 µM at station W and E. Station O always had lower DIP concentrations than stations W and E, particularly during summer, with levels ranging from 0.2–0.4 µM in spring to 0.7–1.0 µM in summer with no specific pattern among years.

Total nitrogen (TN) and phosphorus (TP) in the water column showed irregular patterns driven by wind and waves with station E having consistently higher concentrations than station W and O (Fig. 6). TN was highly irregular and generally dominated (> 50%) by DIN during winter and FPDN during summer. The TP seasonality was similar to that of DIP (Figs. 3), which consistently accounted for about 50% of TP. Accordingly, the FPDP pool followed the same seasonal trend. The excessive peaks in late 2016 were probably a consequence of a storm that caused strong resuspension of surface particles.

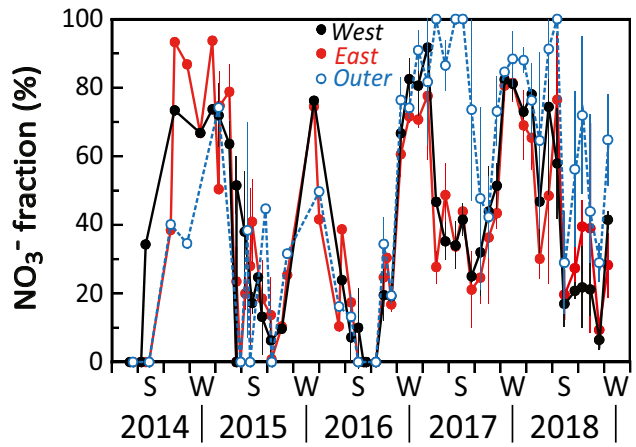

Fig. 5 The contribution of NO_3^- in % of the total DIN pool in lagoon water presented as 1–3-month intervals from May 2014 to June 2016 followed by monthly intervals until January 2019. Black symbols show results from station W; red symbols from station E; and blue symbols from station O. Error bars indicate SE ($n = 3$–5 until June 2016 and $n = 3$ until January 2019)

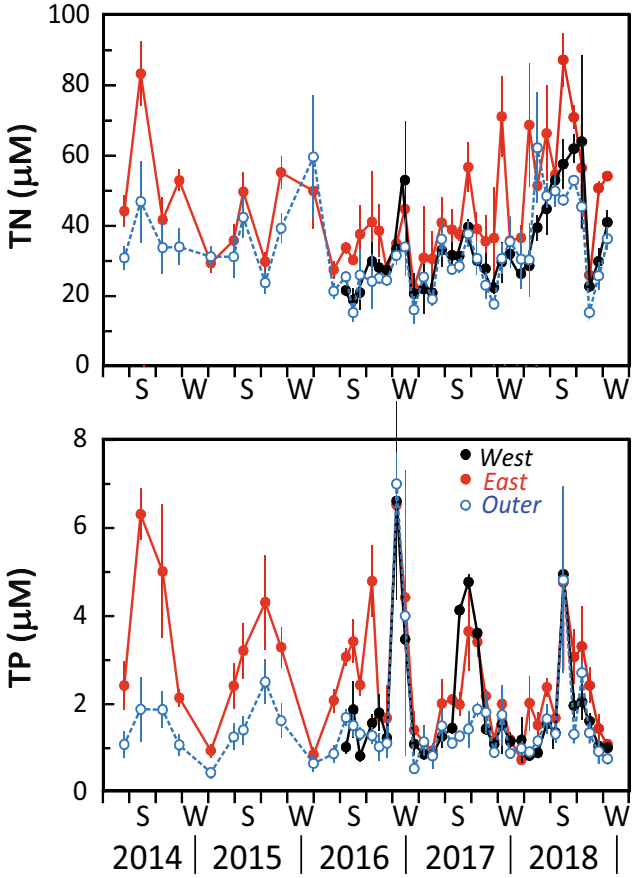

Fig. 6 TN (upper) and TP (lower) concentrations in lagoon water presented as 1–3-month intervals from May 2014 to June 2016 followed by monthly intervals until January 2019. Black symbols show results from station W; red symbols from station E; and blue symbols from station O. Error bars indicate SE ($n = 3$–5 until June 2016 and $n = 3$ until January 2019)

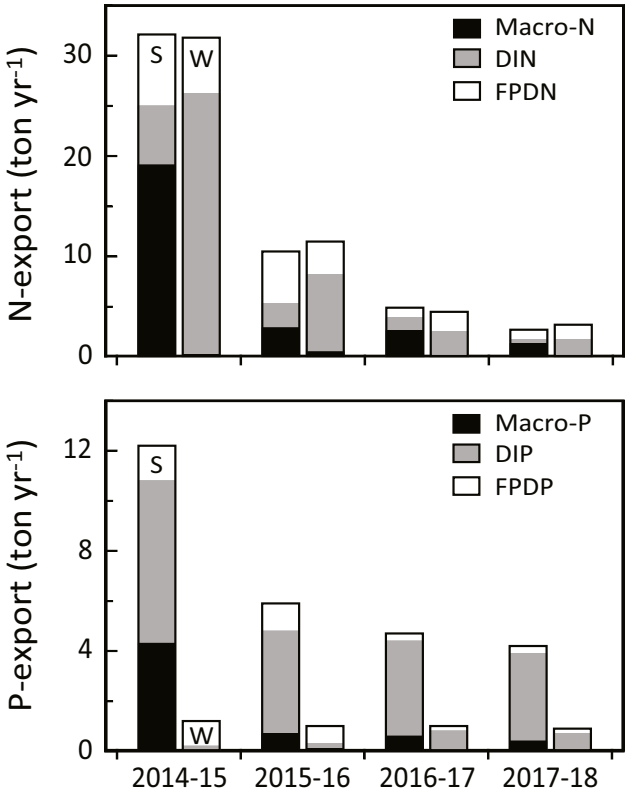

Fig. 7 Export of N and P in the form of macrophyte detritus (Macro-N, Macro-P), dissolved inorganic nitrogen (DIN) and phosphorus (DIP), and fine-particulate and dissolved organic nitrogen (FPDN) and phosphorus (FPDP) from the 214-ha Gyldensteen Coastal Lagoon in 2014–15, 2015–16, 2016–17, and 2017–18. Each year is split into the growth season (S) from April to October and the winter season (W) from November to March

Transport of Macro Detritus

The tidal export of N and P in large particles was high during the growth season (April to October) and very low during the winter season (November to March) in 2014–15 (Fig. 7) and consisted almost entirely of green algal remains. Actually, small amounts (< 1% of the total export) of brown algal (*Fucus* sp.) and eelgrass (*Zostera marina*) detritus was in 2014–15 imported into the Gyldensteen Coastal Lagoon. The net tidal export of macro detritus in the growth season declined rapidly over the years, while it remained very low in the winter season throughout the study period, reaching only an annual total of 18 (N) and 16 (P) % in 2015–16, 14 (N) and 16 (P) % in 2016–17, and 7 (N) and 9 (P) % in 2017–2018 of the macro detritus export in 2014–15. The contribution of green algal detritus also decreased dramatically, and from 2016 and onwards, the export was dominated by *Fucus* sp. detritus and aggregates of cyanobacteria. Green algae contributed at that time with less than 10% of the net N and P export, while *Zostera marina* detritus was always imported in small amounts into the lagoon.

N and P Export

Temporal patterns of N and P loss from flooded soils in the entire 214-ha coastal lagoon showed almost the same trend irrespective of calculation approach despite the inherent high uncertainty in the data of particularly the soil inventory approach (Table 4). Rates were high the first 2 years for N and the first year for P at a level of 22 to 64 ton N yr^{-1} and 6.2 to 13.4 ton P yr^{-1}, respectively, followed by a gradual decrease, which was more pronounced and generally twice as fast for N than P. The first year (2014–15) N and P losses estimated by the soil inventory and model approaches were about two times higher than those obtained by dark fluxes. Subsequently, the difference leveled out and all three approaches showed comparable rates from 2016 to 2019. Both N and P loss therefore appeared to reach a steady level after 1–2 years. The model approach showed that about 30% of the N and P loss the first year (2014–15) consisted of macro detritus, while FPDN and

Table 4 Annual export of N and P by the 214-ha Gyldensteen Coastal Lagoon from summer 2014 to spring 2019 based on three approaches. "Soil" is the area-integrated loss of TN and TP in the upper 20 cm of the soil at 4–6 sites throughout the lagoon. The loss from 2016 to 2018 is split evenly between the 2 years due to lack of 2017 data. "Flux" is the time- and area-integrated average efflux of DIN and DIP measured in darkness at stations W and E. "Model" is the export of dissolved and particulate N and P across the outer boundary modeled from measured DIN, DIP, FPDN, and FPDP concentrations in the water and trapped macro PN and PP using nets. Numbers in parenthesis indicate SD based on the root square sum method (Genereux et al. 2005)

	2014–15	2015–16	2016–17	2017–18	2018–19
Ton N yr^{-1}					
Soil	59.9 (36.9)	50.9 (37.7)	7.5 (19.9)	7.5 (19.9)	-
Flux	33.6 (22.2)	25.1 (11.3)	13.9 (9.9)	9.4 (7.3)	12.6 (6.2)
Model	63.9 (8.2)	22.1 (4.1)	9.4 (2.1)	5.9 (1.2)	-
Ton P yr^{-1}					
Soil	11.9 (19.2)	4.6 (18.5)	4.0 (6.0)	4.0 (6.0)	-
Flux	6.2 (4.0)	3.9 (1.6)	4.9 (2.4)	4.2 (1.9)	3.9 (0.8)
Model	13.4 (2.7)	6.9 (2.2)	5.8 (2.4)	5.1 (1.3)	-

FPDP accounted for about 20% and DIN and DIP contributed with the remaining 50% (Fig. 7). These proportions changed considerably through time and N export in the following 3 years consisted of 16–29% macro detritus, 32–42% FPDN, and 34–46% DIN, while the P proportions were 8–12% macro detritus, 9–26% FPDP, and 62–82% DIP. N export was during all years almost similar in the growth and the winter seasons due to a very high DIN contribution in winter that counteracted the diminished export of macro detritus (Fig. 7). P export, on the other hand, was consistently 5–10 times higher during the growth than the winter season because almost all macro detritus and DIP export occurred during summer.

Discussion

N and P Exchange Patterns and the Underlying Mechanisms

The present study reveals that agricultural soils newly flooded with seawater by managed realignment are substantial sources of N and P to the marine surroundings. The export of both elements is particularly high the first years after flooding, but the subsequent attenuation of soil N loss and release to the overlying water is faster than for P. The available nutrients in flooded agricultural soils originate to a large extent from the large inventory accumulated after many years of intensive fertilization (Bouwman et al. 2013; Muhammed et al. 2018). Accumulated N and P typically occur in the form of labile and refractory organic material (Keller et al. 2002; Alvarez et al. 2018) as well as easily exchangeable (e.g., Fe and clay) and more tightly (e.g., Ca) adsorbed inorganic pools (Romanyà and Rovira 2009; Alvarez et al. 2018). Microbial mineralization, transformation, and exchange of both N and P are relatively fast in non-flooded soil with deep oxygen penetration (Steinmuller et al. 2019). However, the prevailing anoxic conditions in soil submerged by seawater substantially diminish organic matter reactivity (Steinmuller et al. 2019) and adsorption capacity of DIN and DIP, particularly in deeper soils (Mohanty et al. 2013). Accordingly, Sjøgaard et al. (2017) proved that microbial activity in flooded soils from Gyldensteen Coastal Lagoon is largely confined to the upper 5–10 cm and is rapidly declining with time.

DIN and DIP fluxes across marine sediment-water interfaces measured in darkness are generally considered a valid measure of depth-integrated sediment column biogeochemical processes (Kristensen and Hansen 1995; Aller 2014). However, it must be emphasized that a fraction of the DIN and DIP release measured in darkness may be excessive and originate from microbial mineralization and faunal excretion after consuming benthic microalgae produced during preceding periods of light exposure. This artifact may explain the relatively high DIN and DIP release observed from 2016 to 2018 compared with the soil loss and model calculations (Table 4). The initial first year rates of in situ DIN and DIP release from flooded soil to overlying water observed in the present study are comparable with those reported by Valdemarsen et al. (2018) right after experimental flooding of darkened Gyldensteen soils. The subsequent lower dark rates observed after 2015, on the other hand, are similar to those typically observed for DIN and DIP in coastal marine sediments (Kristensen 1993; Dausse et al. 2012; Valdemarsen et al. 2015).

The rapid initial release of DIN is probably caused partly by ion exchange when the concentration of cations, such as Na^+ and Mg^{2+}, increases in the porewater after flooding the soil with seawater. Consequently, NH_4^+ is competitively excluded from negative binding sites in humus and clay particles and released into the porewater (Portnoy and Giblin 1997;

Rysgaard et al. 1999; Ardon et al. 2013). Although this process is instant, the time needed for the metal cations to diffuse downward into and the desorbed NH_4^+ to diffuse upward from 10's of centimeter deep soil layers may be in the order of months to years in the absence of advective porewater transport (Aller 1978; Webster et al. 1996). Accordingly, most of the readily available N-pool is released within the first year, as indicated by the rapid decrease in DIN efflux (Fig. 3) and water column DIN levels the following years (Fig. 4). The decreasing N loss from the soil is not only due to exhaustion of adsorbed NH_4^+ but also a consequence of diminished N mineralization due to declining reactivity of organic-bound N in the flooded anoxic soil (French 2006; Burden et al. 2013; Dale et al. 2019). The lower NH_4^+ availability through time is also evident from the higher proportion of NO_3^- observed in the overlying water (Fig. 5). Thus, slower NH_4^+ release allows time for more complete nitrification in the upper few mm oxic surface soil before NH_4^+ exits to the overlying water. Much of the generated NO_3^- can in turn be lost as N_2 through coupled denitrification in the underlying anoxic soil (Blackwell et al. 2010; Brin et al. 2014) and contribute to the decreasing tidal export of fixed N toward the end of the monitoring period.

A significant portion of soil DIP is adsorbed to Fe (III) hydroxides when not flooded (McDowell and Condron 2001; Dunne et al., 2005), particularly in the upper 20–30-cm thick layer of oxic topsoil in agricultural areas (Tully et al. 2019). Massive desorption of DIP rapidly occurs once anoxic conditions induced by flooding reduces Fe(III) in the topsoil to Fe(II) (Lehtoranta et al. 2015; Tully et al. 2019). DIP desorption is accelerated even further in soils flooded with seawater when sulfides generated by sulfate reduction precipitate and inactivate Fe(II) (Roden and Edmonds 1997; Wu et al. 2019). The diffusion delay of DIP release within flooded soil is typically shorter than for NH_4^+ because the entire soil column, except for the upper few mm, becomes anoxic instantly after flooding (Schreiber et al. 2012; Colmer et al. 2013), leaving only an upward diffusion path before DIP desorbed from Fe is released to the overlying water. This is clearly reflected by the almost instant and rapid post-flooding DIP release at station E in Gyldensteen Coastal Lagoon (Fig. 3) where soil anoxia occurred to the surface under a thick green algal cover in summer 2014 (Thorsen et al. 2019). The lack of similar rapid summer release of DIP at the less macrophyte-covered station W may be caused by a secondary DIP trap in the form of precipitated Fe(III) in the upper oxidized centimeter, which was generated by oxidation of upward diffusing Fe^{2+} not yet trapped by sulfides (Anschutz et al. 2019).

Nevertheless, the rapid DIP desorption and release particularly in the eastern part of the lagoon during the first few months after flooding was responsible for twice as high DIP concentration in the overlying water during summer 2014 than the following summers (Fig. 4). Accordingly, the annual P loss from the coastal lagoon soils decreased from a high level the first year and stabilized at a level half of that the following years. The lack of attenuation in P loss after 2014–15 is intriguing and must be the consequence of a steady release from the large but relatively slow reacting P pools in the flooded agricultural soil. These include residual P bound to other metals than Fe(III) (e.g., Fe^{2+}, Al^{3+}, and Mg^{2+}) that can be released chemically by the continued action of sulfides and elevated pH in the flooded soil (Dijkstra et al. 2016; Tully et al. 2019) and organic P that is mineralized at a steady rate by microorganisms (Kieckbusch and Schrautzer 2007; Kraal et al. 2015). It is perceivable that continued mineralization is a major contributor to the long-term DIP release from flooded soils, since organic P typically represents between 30 and 70% of the total solid P in soils and sediments (Anschutz et al. 2007).

N and P Export

The observed N and P exchange after managed realignment of agricultural soil with seawater reveal a substantial export to the adjacent marine environment during the first years after flooding (Table 4). This result cannot be verified using information from the literature, because no studies have yet made similar N and P estimates immediately following managed realignment of agricultural soil. Data verification must instead rely on the validity of the three independent approaches applied in this study. They provide surprisingly similar trends with an among method variability generally less than a factor of 2 (Table 4), which is satisfactory given the inherent uncertainties in such system-wide export estimates. The consistently lower estimate provided by the flux approach than the inventory and model approach during the first 2 years is probably due to the contribution of dissolved and particulate organic N and P loss detected by the former approach during the very physically, chemically, and biologically dynamic period right after flooding. This is also evident from the high first-year contribution of particulate N and P to the total export out of the lagoon compared with DIN and DIP (Fig. 7). Anyway, the average annual loss and potential export during the first year, as estimated by the three approaches, ranged from 157 to 299 kg N ha^{-1} yr^{-1} and 29 to 63 kg P ha^{-1} yr^{-1} (Table 4). These amounts are in the upper range of or higher than the reported annual fertilizer application (161 kg N ha^{-1} yr^{-1} and 20 kg P ha^{-1} yr^{-1}) to the area during normal cultivation before flooding (Table 1), and considerably higher than the typical annual discharge to the ocean (10–40 kg N ha^{-1} yr^{-1} and 0.1–0.5 kg P ha^{-1} yr^{-1}) via drainage water during cultivation of similar soil types (Øygarden et al. 2014; Clement and Steinman 2017; Hanrahan et al. 2018). Even from 3 to 5 years after flooding, the N and P exports remain substantial, accounting for 28–65 kg N ha^{-1} yr^{-1} and 18–27 kg P ha^{-1} yr^{-1}.

Data on N and P loss from flooded agricultural soils are primarily available from studies where land is converted to freshwater wetlands (e.g., Hoffmann et al. 2011; Kinsman-Costello et al. 2014). Since these wetlands typically receive freshwater from streams rich in DIN, they rarely export N and are not comparable with the N exchange in Gyldensteen Coastal Lagoon. Instead, they are widely used as a tool to mitigate DIN loading into downstream recipients due to intense denitrification within the wetland soil (Hoffmann et al. 2011). Conversely, flooding of historically drained soils and sediments with freshwater may lead to release of Fe-bound P under reducing conditions in the flooded soil. Accordingly, recent studies have reported release of P from newly flooded freshwater wetlands of ~ 30 kg ha^{-1} yr^{-1} (Wong et al. 2011; Kinsman-Costello et al. 2014), which is within the range reported in the present study.

It is remarkable that the decrease in annual P loss from year 2014–15 to 2017–18 was only 32–66%, while annual N loss dropped by 72–91% during the same time period (Table 4). The faster change over time in mobility of soil N than P is also evident from the N:P molar ratio of the loss that decreased from 10.5–12.0 in 2014–15 to 2.6–5.0 in 2017–18. This pattern indicates the presence of a relatively small but highly labile and mobile soil N pool that is released in excess of P during the first years after flooding. A similar pattern with a rapid mobilization of exchangeable N and P pools followed by a rapid decline of particularly the available N pool has been reported after reflooding of saltmarsh sediments (Portnoy and Giblin 1997; Blackwell et al. 2004). The mobile N pool in the flooded Gyldensteen Coastal Lagoon soils may have been spiked excessively by the fertilization with primarily N in the last 2 years before flooding (Table 1). Conversely, the low N:P molar ratio of 3–6 in the Gyldensteen soils indicates a relatively high P content in the flooded agriculture land when compared with ratios of 12–15 reported for unfertilized soils (Cleveland and Liptzin 2007; Alvarez et al. 2018). Interestingly, a small uncultivated patch at Gyldensteen (GI08) showed a similar high soil N:P of 16–18 (Table 3). Part of the large P-pool in the cultivated soils is also mobile, but apparently less so than the labile N-pool that drove the extensive N release during the first couple of years after flooding.

Consequences for the Ecological Status in the Adjacent Marine Environment

The ecological status within coastal lagoons restored by managed realignment of agricultural soil is generally poor the first years after flooding as indicated by the initial unstable and eutrophic conditions in Gyldensteen Coastal Lagoon (Thorsen et al. 2019). The conditions may improve relatively fast, and it appears that the ecological status within a newly flooded lagoon can be considered fair after about 5 years. However, such improvement occurs at the expense of a massive tidal export of N and P to the adjacent water body. If the recipient marine environment is large and with rapid water exchange, as the open Kattegat outside Gyldensteen Coastal Lagoon, the exported nutrients will be diluted almost instantly and not cause eutrophication problems. If, on the other hand, managed realignment of agricultural soil is implemented adjacent to a constrained and already eutrophic water body with low water exchange, the environmental conditions may deteriorate during the first years by the excess nutrient loading.

An example of such eutrophic and sensitive water body surrounded by low-lying reclaimed land is the estuary Mariager Fjord in Denmark (Fallesen et al. 2000). This 35 km long and narrow fjord, that covers an area of 47 km^2, received 800 ton N and 17 ton P per year from land via freshwater discharges in 2011 (Windolf et al. 2013). If managed realignment of similar size and background as Gyldensteen Coastal Lagoon is implemented with discharge to Mariager Fjord, the total N loading will increase by 4–8% during the first year and level out to about 1% after 5 years. The situation for P is more severe with a 36–79% increased discharge the first year and with only a slight decline to about 23% after 5 years. Accordingly, the problem with excess N appears limited even in a small water body and will be almost negligible after a few years, while the augmented P discharge potentially can cause severe problems—particularly when algal growth is P-limited, which typically occurs in spring. It is therefore important to consider the environmental conditions of the adjacent marine recipient carefully before managed realignment of agricultural land is implemented. Small and stagnant water bodies, with particular emphasis on eutrophic and P-limited systems, should be avoided as recipients.

Conclusions

The survey of nutrient export after establishment of Gyldensteen Coastal Lagoon by managed realignment confirmed the first hypothesis that excess nutrients stored in the soil from past fertilization is rapidly lost under the newly flooded anoxic and saline conditions. The faster attenuation of N than P loss during the first 5 years of flooding disproves the second hypothesis, particularly when considering the continued high loss of P. The potential wider impact of the high N and P exports depends on the water residence time and volume of the recipient marine ecosystem. In the case of Gyldensteen Coastal Lagoon where the excess nutrients are discharged into an open marine environment with rapid water exchange, the eutrophication impact must be considered limited. If a similar managed realignment project is implemented adjacent to a constrained and eutrophic water body near its "tipping point," the high and extended discharge of particularly P may be ecologically detrimental for several years.

Acknowledgments We are grateful for skillful laboratory assistance by B. Christensen, K.C. Kirkegaard, and R.O. Holm, as well as several engaged students over the years.

Funding Information This research was funded by the Aage V. Jensen Nature Foundation.

References

Aller, R.C. 1978. Experimental studies of changes produced by deposit feeders on pore water, sediment, and overlying water chemistry. *American Journal of Science* 278 (9): 1185–1234.

Aller, R.C. 2014. Sedimentary diagenesis, depositional environments, and benthic fluxes. In *Treatise on geochemistry*, ed. H.D. Holland and K.K. Turekian, vol. 8, Second ed., 293–334. Oxford: Elsevier.

Alvarez, R., A. Gimenez, M.M. Caffaro, F. Pagnanini, V. Recondo, C.D. Molina, G. Berhongaray, M.R. Mendoza, D.A. Ramil, F. Facio, J.L. De Paepe, H.S. Steinbach, and R.J. Cantet. 2018. Land use affected nutrient mass with minor impact on stoichiometry ratios in Pampean soils. *Nutrient Cycling in Agroecosystems* 110 (2): 257–276.

Andrews, J.E., G. Samways, and G.B. Shimmield. 2008. Historical storage budgets of organic carbon, nutrient and contaminant elements in saltmarsh sediments: Biogeochemical context for managed realignment, Humber Estuary, UK. *Science of the Total Environment* 405 (1-3): 1–13.

Anschutz, P., G. Chaillou, and P. Lecroart. 2007. Phosphorus diagenesis in sediment of the Thau Lagoon. *Estuarine, Coastal and Shelf Science* 72 (3): 447–456.

Anschutz, P., S. Bouchet, G. Abril, R. Bridou, E. Tessier, and D. Amouroux. 2019. In vitro simulation of oscillatory redox conditions in intertidal sediments: N, Mn, Fe, and P coupling. *Continental Shelf Research* 177: 33–41.

Ardón, M., J.L. Morse, B.P. Colman, and E.S. Bernhardt. 2013. Drought-induced saltwater incursion leads to increased wetland nitrogen export. *Global Change Biology* 19 (10): 2976–2985.

Ardón, M., A.M. Helton, M.D. Scheuerell, and E.S. Bernhardt. 2017. Fertilizer legacies meet saltwater incursion: Challenges and constraints for coastal plain wetland restoration. *Elementa Science of the Anthropocene* 5: 41. https://doi.org/10.1525/elementa.236.

Arnbjerg-Nielsen, K., L. Leonardsen, and H. Madsen. 2015. Evaluating adaptation options for urban flooding based on new high-end emission scenario regional climate model simulations. *Climate Research* 64 (1): 73–84.

Blackwell, M.S.A., D.V. Hogan, and E. Maltby. 2004. The short-term impact of managed realignment on soil environmental variables and hydrology. *Estuarine, Coastal and Shelf Science* 59 (4): 687–701.

Blackwell, M.S.A., S. Yamulki, and R. Bol. 2010. Nitrous oxide production and denitrification rates in estuarine intertidal saltmarsh and managed realignment zones. *Estuarine, Coastal and Shelf Science* 87 (4): 591–600.

Bouwman, L., K.K. Goldewijk, K.W. Van Der Hoek, A.H.W. Beusen, D.P. Van Vuuren, J. Willems, M.C. Rufino, and E. Stehfest. 2013. Exploring global changes in nitrogen and phosphorus cycles in agriculture induced by livestock production over the 1900–2050 period. *Proceedings of the National Academy of Sciences* 110 (52): 20882–20887.

Brady, A.F., and C.S. Boda. 2017. How do we know if managed realignment for coastal habitat compensation is successful? Insights from the implementation of the EU Birds and Habitats Directive in England. *Ocean & Coastal Management* 143: 164–174.

Brin, L.D., A.E. Giblin, and J.J. Rich. 2014. Environmental controls of anammox and denitrification in southern New England estuarine and shelf sediments. *Limnology and Oceanography* 59 (3): 851–860.

Burden, A., R.A. Garbutt, C.D. Evans, D.L. Jones, and D.M. Cooper. 2013. Carbon sequestration and biogeochemical cycling in a saltmarsh subject to coastal managed realignment. *Estuarine, Coastal and Shelf Science* 120: 12–20.

Burton, E.D., R.T. Bush, S.G. Johnston, L.A. Sullivan, and A.F. Keene. 2011. Sulfur biogeochemical cycling and novel Fe–S mineralization pathways in a tidally re-flooded wetland. *Geochimica et Cosmochimica Acta* 75 (12): 3434–3451.

Chapman, P.M. 2017. Assessing and managing stressors in a changing marine environment. *Marine Pollution Bulletin* 124 (2): 587–590.

Clavero, V., J.J. Izquierdo, J.A. Fernandez, and F.X. Niell. 2000. Seasonal fluxes of phosphate and ammonium across the sediment-water interface in a shallow small estuary (Palmones River, southern Spain). *Marine Ecology Progress Series* 198: 51–60.

Clement, D.R., and A.D. Steinman. 2017. Phosphorus loading and ecological impacts from agricultural tile drains in a west Michigan watershed. *Journal of Great Lakes Research* 43 (1): 50–58.

Cleveland, C.C., and D. Liptzin. 2007. C:N:P stoichiometry in soil: Is there a "Redfield ratio" for the microbial biomass? *Biogeochemistry* 85 (3): 235–252.

Colmer, T.D., O. Pedersen, A.M. Wetson, and T.J. Flowers. 2013. Oxygen dynamics in a salt-marsh soil and in *Suaeda maritima* during tidal submergence. *Environmental and Experimental Botany* 92: 73–82.

Dale, J., H.M. Burgess, and A.B. Cundy. 2017. Sedimentation rhythms and hydrodynamics in two engineered environments in an open coast managed realignment site. *Marine Geology* 383: 120–131.

Dale, J., A.B. Cundy, K.L. Spencer, S.J. Carr, I.W. Croudace, H.M. Burgess, and D.J. Nash. 2019. Sediment structure and physicochemical changes following tidal inundation at a large open coast managed realignment site. *Science of the Total Environment* 660: 1419–1432.

Dausse, A., A. Garbutt, L. Norman, S. Papadimitriou, L.M. Jones, P.E. Robins, and D.N. Thomas. 2012. Biogeochemical functioning of grazed estuarine tidal marshes along a salinity gradient. *Estuarine, Coastal and Shelf Science* 100: 83–92.

Dijkstra, N., C.P. Slomp, and T. Behrends. 2016. Vivianite is a key sink for phosphorus in sediments of the Landsort Deep, an intermittently anoxic deep basin in the Baltic Sea. *Chemical Geology* 438: 58–72.

Dunne, E.J., N. Culleton, G. O'Donovan, R. Harrington, and K. Daly. 2005. Phosphorus retention and sorption by constructed wetland soils in Southeast Ireland. *Water Research* 39 (18): 4355–4362.

Esteves, L. S. 2014. Managed realignment: A viable long-term coastal management strategy? SpringerBriefs in Environmental Science, DOI https://doi.org/10.1007/978-94-017-9029-1_1. Springer Science+Business Media, Dordrecht.

Etheridge, J.R., F. Birgand, and M.R. Burchell. 2015. Quantifying nutrient and suspended solids fluxes in a constructed tidal marsh following rainfall: The value of capturing the rapid changes in flow and concentrations. *Ecological Engineering* 78: 41–52.

Fallesen, G., F. Andersen, and B. Larsen. 2000. Life, death and revival of the hypertrophic Mariager Fjord, Denmark. *Journal of Marine Systems* 25 (3-4): 313–321.

Fenger, J., E. Buch, P.R. Jakobsen, and P. Vestergaard. 2008. Danish attitudes and reactions to the threat of sea-level rise. *Journal of Coastal Research* 24: 394–402.

Flindt, M.R., and L. Kamp-Nielsen. 1997. Modelling an estuarine eutrophication gradient. *Ecological Modelling* 102 (1): 143–154.

Flindt, M., J. Salomonsen, M. Carrer, M. Bocci, and L. Kamp-Nielsen. 1997. Loss, growth and transport dynamics of *Chaetomorpha aerea* and *Ulva rigida* in the Lagoon of Venice during an early summer field campaign. *Ecological Modelling* 192: 133–141.

Flindt, M.R., J. Neto, C.L. Amos, M.A. Pardal, A. Bergamasco, C.B. Pedersen, and F.Ø. Andersen. 2004 Plant bound nutrient transport.

Mass transport in estuaries and lagoons In Estuarine nutrient cycling: The influence of primary producers, eds. S.L. Nielsen, G.T. Banta, and M.F. Pedersen. Aquatic Ecology Book Series, vol 2. Dordrecht: Springer.

French, P.W. 2006. Managed realignment - The developing story of a comparatively new approach to soft engineering. *Estuarine, Coastal and Shelf Science* 67 (3): 409–423.

Hale, S.S., G. Cicchetti, and C.F. Deacutis. 2016. Eutrophication and hypoxia diminish ecosystem functions of benthic communities in a New England estuary. *Frontiers in Marine Science* 3: 249. https://doi.org/10.3389/fmars.2016.00249.

Hall, J.W., P.B. Sayers, M.J.A. Walkden, and M. Panzeri. 2006. Impacts of climate change on coastal flood risk in England and Wales: 2030-2100. *Philosophical Transactions of the Royal Society A* 364 (1841): 1027–1049.

Hanrahan, B.R., J.L. Tank, S.F. Christopher, U.H. Mahl, M.T. Trentman, and T.V. Royer. 2018. Winter cover crops reduce nitrate loss in an agricultural watershed in the central U.S. *Agriculture, Ecosystems and Environment* 265: 513–523.

Hansen, K. 2008. Det Tabte Land – Den store fortælling om magten over det danske landskab (in Danish). Copenhagen: Gads Forlag.

Hansen, K. 2014. *Folk & fortællinger fra det tabte land – Øerne (in Danish)*. Klippinge: Forlaget Bæredygtighed.

Hansen, L. 2018. Sea level data 1889–2017 from 14 stations in Denmark. DMI Report 18–16.

Heyburn, J., P. McKenzie, M.J. Crawley, and D.A. Fornara. 2017. Effects of grassland management on plant C:N:P stoichiometry: Implications for soil element cycling and storage. *Ecosphere* 8 (10): e01963. https://doi.org/10.1002/ecs2.1963.

Hoffmann, C.C., B. Kronvang, and J. Audet. 2011. Evaluation of nutrient retention in four restored Danish riparian wetlands. *Hydrobiologia* 674 (1): 5–24.

IPCC. 2014. Climate change 2014: Synthesis report. Contribution of Working Groups I, II and III to the fifth assessment report of the Intergovernmental Panel on Climate Change. World Meteorological Organization. Geneva.

IPCC. 2019. Summary for policymakers. In: IPCC Special Report on the Ocean and Cryosphere in a Changing Climate. Geneva.

Keller, T., A. Trautner, and J. Arvidsson. 2002. Stress distribution and soil displacement under a rubber-tracked and a wheeled tractor during ploughing, both on-land and within furrows. *Soil & Tillage Research* 68 (1): 39–47.

Kieckbusch, J.J., and J. Schrautzer. 2007. Nitrogen and phosphorus dynamics of a re-wetted shallow-flooded peatland. *Science of the Total Environment* 380 (1-3): 3–12.

Kinsman-Costello, L.E., J. O'Brien, and S.K. Hamilton. 2014. Re-flooding a historically drained wetland leads to rapid sediment phosphorus release. *Ecosystems* 17 (4): 641–656. https://doi.org/10.1007/s10021-014-9748-6.

Koroleff, F. 1983. Determination of phosphorus. In *Methods of seawater analysis*, ed. K. Grashof, M. Erhardt, and K. Kremling, 125–131. Weinheim: Verlag Chemie.

Kraal, P., E.D. Burton, A.L. Rose, B.D. Kocar, R.S. Lockhart, K. Grice, R.T. Bush, E. Tan, and S.M. Webb. 2015. Sedimentary iron–phosphorus cycling under contrasting redox conditions in a eutrophic estuary. *Chemical Geology* 392: 19–31.

Kristensen, E. 1993. Seasonal variations in benthic community metabolism and nitrogen dynamics in a shallow, organic-poor Danish lagoon. *Estuarine, Coastal and Shelf Science* 36 (6): 565–586.

Kristensen, E., and K. Hansen. 1995. Decay of plant detritus in organic-poor marine sediment: Production rates and stoichiometry of dissolved C and N compounds. *Journal of Marine Research* 53 (4): 675–702.

Lefcheck, J.S., R.J. Orth, W.C. Dennison, D.J. Wilcox, R.R. Murphy, J. Keisman, C. Gurbisz, M. Hannam, J.B. Landry, K.A. Moore, C.J. Patrick, J. Testa, D.E. Weller, and R.A. Batiuk. 2017. Long-term nutrient reductions lead to the unprecedented recovery of a temperate coastal region. *Proceedings of the National Academy of Sciences* 115: 3658–3366.

Lehtoranta, J., P. Ekholm, S. Wahlström, P. Tallberg, and R. Uusitalo. 2015. Labile organic carbon regulates phosphorus release from eroded soil transported into anaerobic coastal systems. *Ambio* 44 (Suppl. 2): S263–S273.

Mander, L., L. Marie-Orleach, and M. Elliott. 2013. The value of wader foraging behaviour study to assess the success of restored intertidal areas. *Estuarine, Coastal and Shelf Science* 131: 1–5.

McDowell, R., and L. Condron. 2001. Influence of soil constituents on soil phosphorus sorption and desorption. *Communications in Soil Science and Plant Analysis* 32 (15-16): 2531–2547.

Meier, H.E.M., A. Höglund, K. Eilola, and E. Almroth-Rosell. 2017. Impact of accelerated future global mean sea level rise on hypoxia in the Baltic Sea. *Climate Dynamics* 49 (1-2): 163–172.

Mohanty, S., A.K. Nayak, A. Kumar, R. Tripathi, M. Shahid, P. Bhattacharyya, R. Raja, and B.B. Panda. 2013. Carbon and nitrogen mineralization kinetics in soil of rice-rice system under long term application of chemical fertilizers and farmyard manure. *European Journal of Soil Biology* 58: 113–121.

Muhammed, S.E., K. Coleman, L. Wu, V.A. Bell, J.A.C. Davies, J.N. Quinton, E.J. Carnell, S.J. Tomlinson, A.J. Dore, U. Dragosits, P.S. Naden, M.J. Glendining, E. Tipping, and A.P. Whitmore. 2018. Impact of two centuries of intensive agriculture on soil carbon, nitrogen and phosphorus cycling in the UK. *Science of the Total Environment* 634: 1486–1504.

Nash, J.E., and J.V. Sutcliffe. 1970. River flow forecasting through conceptual models. Part I — A discussion of principles. *Journal of Hydrology* 10: 282–290.

Øygarden, L., J. Deelstra, A. Lagzdins, M. Bechmann, I. Greipsland, K. Kyllmar, A. Povilaitis, and A. Iital. 2014. Climate change and the potential effects on runoff and nitrogen losses in the Nordic–Baltic region. *Agriculture, Ecosystems and Environment* 198: 114–126.

Paerl, H.W., N.S. Hall, B.L. Peierls, and K.L. Rossignol. 2014. Evolving paradigms and challenges in estuarine and coastal eutrophication dynamics in a culturally and climatically stressed world. *Estuaries and Coasts* 37 (2): 243–258.

Pétillon, J., S. Potier, A. Carpentier, and A. Garbutt. 2014. Evaluating the success of managed realignment for the restoration of salt marshes: Lessons from invertebrate communities. *Ecological Engineering* 69: 70–75.

Portnoy, J.W., and A.E. Giblin. 1997. Biogeochemical effects of seawater restoration to diked salt marshes. *Ecological Applications* 7 (3): 1054–1063.

Roden, E.E., and J.W. Edmonds. 1997. Phosphate mobilization in iron-rich anaerobic sediments: Microbial Fe(III) oxide reduction versus iron-sulfide formation. *Archiv für Hydrobiologie* 139: 347–378.

Romanyà, J., and P. Rovira. 2009. Organic and inorganic P reserves in rain-fed and irrigated calcareous soils under long-term organic and conventional agriculture. *Geoderma* 151 (3-4): 378–386.

Rupp-Armstrong, S., and R.J. Nicholls. 2007. Coastal and estuarine retreat: A comparison of the application of managed realignment in England and Germany. *Journal of Coastal Research* 23: 1418–1430.

Rysgaard, S., P. Thastum, T. Dalsgaard, P.B. Christensen, and N.P. Sloth. 1999. Effects of salinity on NH_4^+ adsorption capacity, nitrification, and denitrification in Danish estuarine sediments. *Estuaries* 22 (1): 21–30.

Schreiber, C.M., B. Zeng, S. Blossfeld, U. Rascher, M. Kazda, U. Schurr, A. Höltkemeier, and A.J. Kuhn. 2012. Monitoring rhizospheric pH, oxygen, and organic acid dynamics in two short-time flooded plant species. *Journal of Plant Nutrition and Soil Science* 175 (5): 761–768.

Schuerch, M., T. Spencer, S. Temmerman, M.L. Kirwan, C. Wolff, D. Lincke, C.J. McOwen, M.D. Pickering, R. Reef, A.T. Vafeidis, J.

Hinkel, R.J. Nicholls, and S. Brown. 2018. Future response of global coastal wetlands to sea-level rise. *Nature* 561 (7722): 231–234.

Serpetti, N., U.F.M. Witte, and M.R. Heath. 2016. Statistical modeling of variability in sediment-water nutrient and oxygen fluxes. *Frontiers in Earth Science* 4: 65. https://doi.org/10.3389/feart.2016.00065.

Sjøgaard, K.S., A.H. Treusch, and T.B. Valdemarsen. 2017. Carbon degradation in agricultural soils flooded with seawater after managed coastal realignment. *Biogeosciences* 14 (18): 4375–4389.

Smith, S.L., S.E. Cunniff, N.S. Peyronnin, and J.P. Kritzera. 2017. Prioritizing coastal ecosystem stressors in the Northeast United States under increasing climate change. *Environmental Science and Policy* 78: 49–57.

Spencer, K.L., S.J. Carr, L.M. Diggens, J.A. Tempest, M.A. Morris, and G.L. Harvey. 2017. The impact of pre-restoration land-use and disturbance on sediment structure, hydrology and the sediment geochemical environment in restored saltmarshes. *Science of the Total Environment* 587–588: 47–58.

Steinmuller, H.E., K.M. Dittmer, J.R. White, and L.G. Chambers. 2019. Understanding the fate of soil organic matter in submerging coastal wetland soils: A microcosm approach. *Geoderma* 337: 1267–1277.

Stenak, M. 2005. *De inddæmmede landskaber – en historisk geografi (in Danish)*. Auning: Landbohistorisk Selskab.

Stookey, L.L. 1970. Ferrozine - A new spectrophotometric reagent for iron. *Analytical Chemistry* 42 (7): 779–781.

Thorsen, S.W., E. Kristensen, T. Valdemarsen, M.R. Flindt, C.O. Quintana, and M. Holmer. 2019. Fertilizer-derived N in opportunistic macroalgae after flooding of agricultural land. *Marine Ecology Progress Series* 616: 37–49.

Tully, K.L., D. Weissman, W.J. Wyner, J. Miller, and T. Jordan. 2019. Soils in transition: Saltwater intrusion alters soil chemistry in agricultural fields. *Biogeochemistry* 142 (3): 339–356.

Valdemarsen, T., C.O. Quintana, M.R. Flindt, and E. Kristensen. 2015. Organic N and P in eutrophic fjord sediments – Rates of mineralization and consequences for internal nutrient loading. *Biogeosciences* 12: 1–15.

Valdemarsen, T., C.O. Quintana, S.W. Thorsen, and E. Kristensen. 2018. Benthic macrofauna bioturbation and early colonization in newly flooded coastal habitats. *PLoS ONE* 13 (4): e0196097. https://doi.org/10.1371/journal.pone.0196097.

Vousdoukas, M.I., L. Mentaschi, E. Voukouvalas, A. Bianchi, F. Dottori, and L. Feyen. 2018. Climatic and socioeconomic controls of future coastal flood risk in Europe. *Nature Climate Change* 8 (9): 776–780.

Webster, I.T., S.J. Norquay, F.C. Ross, and R.A. Wooding. 1996. Solute exchange by convection within estuarine sediments. *Estuarine, Coastal and Shelf Science* 42 (2): 171–183.

Wessel, B.M., E. Kristensen, and M.C. Rabenhorst. 2019. Changing tides: Land reclamation and lagoon restoration in Gyldensteen Strand, Denmark, soil science Society of America Annual Meeting, San Diego, CA, January 6–9. Oral.

Windolf, J., A. Timmermann, A. Kjeldgaard, J. Bøgestrand, Larsen, S.L., and H. Thodsen. 2013. Landbaseret tilførsel af kvælstof og fosfor til danske fjorde og kystafsnit, 1990–2011 (in Danish). *Technical Report no 31 from the Danish National Centre for Environment and Energy* (http://dce2.au.dk/pub/TR31.pdf).

Wironen, M.B., E.M. Bennett, and J.D. Erickson. 2018. Phosphorus flows and legacy accumulation in an animal-dominated agricultural region from 1925 to 2012. *Global Environmental Change* 50: 88–99.

Wong, S.W., M.J. Barry, A.R. Aldous, N.T. Rudd, H.A. Hendrixson, and C.M. Doehring. 2011. Nutrient release from a recently flooded delta wetland: Comparison of field measurements to laboratory results. *Wetlands* 31 (2): 433–443.

Woodruff, J.D., J.L. Irish, and S.J. Camargo. 2013. Coastal flooding by tropical cyclones and sea-level rise. *Nature* 504 (7478): 44–52.

Wu, S., Y. Zhao, Y. Chen, X. Dong, M. Wang, and G. Wang. 2019. Sulfur cycling in freshwater sediments: A cryptic driving force of iron deposition and phosphorus mobilization. *Science of the Total Environment* 657: 1294–1303.